Physics Letters B 784 (2018) 397–404

Contents lists available at ScienceDirect

Physics Letters B

www.elsevier.com/locate/physletb

Next-to-next-to-leading order N-jettiness soft function for tW production

Hai Tao Li [a], Jian Wang [b,*]

[a] Los Alamos National Laboratory, Theoretical Division, Los Alamos, NM 87545, USA
[b] Physik Department T31, Technische Universität München, James-Franck-Straße 1, D-85748 Garching, Germany

ARTICLE INFO

Article history:
Received 6 June 2018
Received in revised form 7 August 2018
Accepted 13 August 2018
Available online 14 August 2018
Editor: J. Hisano

ABSTRACT

We calculate the N-jettiness soft function for tW production up to next-to-next-to-leading order in QCD, which is an important ingredient of the N-jettiness subtraction method for predicting the differential cross sections of massive colored particle productions. The divergent parts of the results have been checked using the renormalization group equations controlled by the soft anomalous dimension.

1. Introduction

Precise calculation of cross sections for the processes at the Large Hadron Collider (LHC) or future high-energy hadron colliders is crucial for testing the Standard Model (SM) and for searching for new physics. In the last a few years, there is a burst of fully differential next-to-next-to-leading order (NNLO) results for a large number of processes in the SM; see a recent review in ref. [1]. One of the main difficulties in the higher-order QCD calculations is to develop a systematical method to deal with the infrared singularities caused by double real emissions. The N-jettiness subtraction [2,3] has proven to be successful in computing the NNLO differential cross sections of processes with jets, for example, $W/Z/H/\gamma + j$ [2,4–6]. This subtraction method is based on the soft-collinear effective theory (SCET) [7–11], which is an effective theory of QCD in the infrared regions. The N-jettiness $\mathcal{T}_N$ is an observable, proposed in [12], to describe the event shape of jet processes or processes with initial-state hadrons, a generalization of thrust at lepton colliders and beam thrust at hadron colliders [13]. The application of this observable to the NNLO calculations has been explored extensively for massive quark decay [14], and differential cross sections of processes at both hadron colliders [2–6,15,16] and electron-hadron colliders [17,18]. It is also used as a jet resolution variable in combining higher-order resummation with NLO calculations and parton showers [19]. However, for more complicated processes, e.g., involving one massive and two massless partons, the results are still missing.

The N-jettiness event shape variable is defined by [12]

$$\mathcal{T}_N = \sum_k \min_i \{n_i \cdot q_k\} \ , \tag{1}$$

where n_i $(i = a, b, 1, ..., N)$ are light-like reference vectors representing the moving directions of massless external particles, and q_k denotes the momentum of soft or collinear partons. Note that eq. (1) seems different from the original definition in ref. [12] because the variable $\mathcal{T}_N$ in our definition is of mass dimension one while that in ref. [12] is dimensionless. But they are actually the same up to a constant factor Q after replacing n_i by $2q_i/Q$. In the infrared divergent regions, the observable $\mathcal{T}_N \to 0$, and the cross section is approximated by [12,13]

$$\frac{d\sigma}{d\mathcal{T}_N} \propto \int H \otimes B_1 \otimes B_2 \otimes S \otimes \left(\prod_{n=1}^{N} J_n \right) . \tag{2}$$

Here the hard function H encodes all the information about hard scattering. The beam functions B_i, $(i = 1, 2)$, describe the perturbative and non-perturbative contributions from initial state, and have been obtained up to NNLO [20–23]. The jet function J_n describes the final-state jet with a fixed invariant mass and has been calculated at NNLO [24,25]. The soft function S contains soft interactions between all colored particles. It has been studied up to NNLO for massless processes [26–31].

The differential cross section for any observable $\mathcal{O}$ is given by

$$\frac{d\sigma}{d\mathcal{O}} = \frac{d\sigma}{d\mathcal{O}}\Big|_{\mathcal{T}_N < \Delta} + \frac{d\sigma}{d\mathcal{O}}\Big|_{\mathcal{T}_N > \Delta} , \tag{3}$$

where a small cut-off parameter Δ on the right-hand side is imposed. For the NNLO calculations the first term on the right-hand

* Corresponding author.
E-mail addresses: haitaoli@lanl.gov (H.T. Li), j.wang@tum.de (J. Wang).

https://doi.org/10.1016/j.physletb.2018.08.019

side at the leading power can be obtained by expanding eq. (2) to the second order of the strong coupling α_s. The second term, due to the phase-space constraint, can be dealt with the standard NLO subtraction method for the process with an extra parton in the final state.

The extension of the N-jettiness subtraction to more complicated processes requires the calculation of the corresponding soft and hard functions. We have calculated the N-jettiness soft function for one massive colored particle production up to NNLO in ref. [32], where we assume that it is produced at rest. In this paper, we present the result for more general situations, i.e., the massive colored particle can carry any possible momentum. Our result can be used to construct the N-jettiness subtraction terms for tW production at hadron colliders.

This paper is organized as follows. In section 2, we briefly introduce the definition of the soft function in terms of soft Wilson lines. In section 3, we study the renormalization group (RG) equation of the soft function and thus derive the structure of the soft function. We provide the details of the techniques in our calculations in section 4. Then, in section 5, we present the numerical results of the NLO and NNLO soft functions and compare the divergent terms with the predictions from RG equation. We conclude in section 6.

2. Definition of the soft function

In this section we first discuss the kinematics and the factorization of the cross section for tW production. Then we present the definition of soft function.

We consider the process

$$P_1 + P_2 \to t/\bar{t} + W^{\pm} + X\,, \tag{4}$$

where P_1 and P_2 denote incoming hadrons, $t/\bar{t}$ and $W^{\pm}$ represent the top/anti-top quark and the W-boson in the final state, respectively. And X includes any unobserved final state. The partonic process at leading order (LO) for tW^- production is

$$b(p_1) + g(p_2) \to t(p_3) + W^-(p_4)\,. \tag{5}$$

It is convenient to introduce two light-like vectors

$$n^\mu = (1,0,0,1), \qquad \bar{n}^\mu = (1,0,0,-1)\,. \tag{6}$$

Any momentum can be decomposed as $p^\mu = (p^+, p^-, p_\perp)$ with $p^+ = p\cdot n$, $p^- = p\cdot\bar{n}$. The momenta given in eq. (5) can be written in the partonic center-of-mass frame as

$$p_1^\mu = \frac{\sqrt{\hat{s}}}{2}n^\mu\,, \quad p_2^\mu = \frac{\sqrt{\hat{s}}}{2}\bar{n}^\mu, \quad p_3^\mu = m_t v^\mu\,, \tag{7}$$

where $v^2 = 1$. Specifically, we parameterize v by two variables, i.e., β_t and θ_t, which measure the magnitude and the direction of the velocity,

$$v^+ = \frac{1-\beta_t\cos\theta_t}{\sqrt{1-\beta_t^2}}, \quad v^- = \frac{1+\beta_t\cos\theta_t}{\sqrt{1-\beta_t^2}}, \quad |v_\perp| = \frac{\beta_t\sin\theta_t}{\sqrt{1-\beta_t^2}}, \tag{8}$$

where $\beta_t = \sqrt{1-m_t^2/E_t^2}$ with E_t the top quark energy. The 0-jettiness event shape variable in this process is defined as

$$\tau \equiv \mathcal{T}_0 = \sum_k \min\{n\cdot q_k, \bar{n}\cdot q_k\}\,. \tag{9}$$

Since $n\cdot q_k \equiv 2p_1\cdot q_k/\sqrt{\hat{s}}$ and $\bar{n}\cdot q_k \equiv 2p_2\cdot q_k/\sqrt{\hat{s}}$, this definition of τ is Lorentz invariant. The explicit choice in eq. (6) just makes our calculation easier, but the final result is general and independent of this choice.

In the limit $\tau \ll \sqrt{\hat{s}}$, the final state contains no hard radiations, only soft and collinear radiations allowed. In this limit the cross section admits a factorised form, which can be derived in the framework of SCET. For tW production, the collinear singularities, which are only associated with the initial partons, and the soft singularities are all properly regularised by τ defined in eq. (9). Compared with processes without massive colored particles, the only difference is the soft function and the hard function. Following [12,13], we write

$$\begin{aligned}\frac{d\sigma}{dY d\tau} = &\int d\Phi_2 \frac{d\hat{\sigma}_0}{d\Phi_2}\int dt_a dt_b d\tau_s \\ &\times H(\beta_t,\cos\theta_t,\mu) B_1(t_a,x_a,\mu) B_2(t_b,x_b,\mu) \\ &\times S(\tau_s,\beta_t,\cos\theta_t,\mu)\delta\left(\tau-\tau_s-\frac{t_a+t_b}{\sqrt{\hat{s}}}\right)\left(1+\mathcal{O}\left(\frac{\tau}{\sqrt{\hat{s}}}\right)\right)\,,\end{aligned} \tag{10}$$

where $\int d\Phi_2$ is the two-body phase space integral, $d\hat{\sigma}_0$ is the LO partonic differential cross section, Y is the rapidity of the partonic colliding system in the laboratory frame, the momentum fractions $x_a = \sqrt{\hat{s}/s}e^Y$ and $x_b = \sqrt{\hat{s}/s}e^{-Y}$ with $\sqrt{s}$ the collider energy, and μ is the renormalization scale. In momentum space the soft function is defined as the vacuum matrix element

$$\begin{aligned}S(\tau,\beta_t,\cos\theta_t,\mu) = &\sum_{X_s}\left\langle 0\left|\bar{\mathbf{T}}Y_n^\dagger Y_{\bar{n}} Y_v\right|X_s\right\rangle \\ &\times\delta\left(\tau-\sum_k\min\left(n\cdot\hat{P}_k,\bar{n}\cdot\hat{P}_k\right)\right)\left\langle X_s\left|\mathbf{T}Y_n Y_{\bar{n}}^\dagger Y_v^\dagger\right|0\right\rangle,\end{aligned} \tag{11}$$

where $\mathbf{T}(\bar{\mathbf{T}})$ is the (anti-)time-ordering operator. And Y_n, $Y_{\bar{n}}$ and Y_v are the soft Wilson lines defined explicitly as [10,33,34]

$$Y_n(x) = \mathbf{P}\exp\left(ig_s\int_{-\infty}^0 ds\, n\cdot A_s^a(x+sn)\mathbf{T}^a\right), \tag{12}$$

$$Y_{\bar{n}}^\dagger(x) = \bar{\mathbf{P}}\exp\left(-ig_s\int_{-\infty}^0 ds\,\bar{n}\cdot A_s^a(x+s\bar{n})\mathbf{T}^a\right), \tag{13}$$

$$Y_v^\dagger(x) = \mathbf{P}\exp\left(ig_s\int_0^\infty ds\, v\cdot A_s^a(x+sv)\mathbf{T}^a\right) \tag{14}$$

where $\mathbf{P}$ and $\bar{\mathbf{P}}$ are the path-ordering and the anti-path-ordering operators. $\hat{P}_k$ in eq. (11) is the operator extracting the momentum of each soft emission. The purpose of this paper is to calculate the soft function defined above for tW production up to NNLO accuracy.

3. Renormalization

In SCET the bare soft function in eq. (11) contains ultra-violet divergences in perturbative calculations, which are cancelled by the counterterm defined in the standard renormalization procedure. The renormalized soft function is finite and can be used in the calculation of the cross section in eq. (10). The renormalization introduces the scale μ dependence in the soft function, as well as in the hard and beam function. Because of the fact that the physical cross section does not dependent on the intermediate scale, the RG equation of the soft function can be derived from the RG equations of the hard and beam function, which will be used to extract

the anomalous dimension of the soft function. Given the anomalous dimension the divergences in the bare soft function, as well as the scale dependence of the renormalized soft function, can be predicted. In this section we briefly discuss the renormalization of the soft function and the expression of the soft anomalous dimension. We work in $d = 4 - 2\epsilon$ dimensional space-time.

Based on dimensional analysis, the bare soft function, in perturbation theory, can be written as

$$\begin{aligned} &S(\tau, \beta_t, \cos\theta_t, \mu) \\ &= \delta(\tau) + \frac{1}{\tau}\sum_{n=1}^{\infty}\left(\frac{Z_{\alpha_s}\alpha_s}{4\pi}\right)^n \left(\frac{\tau}{\mu}\right)^{-2n\epsilon} s^{(n)}(\beta_t, \cos\theta_t)\,, \end{aligned} \tag{15}$$

where we use renormalized strong coupling α_s and its renormalization factor $Z_{\alpha_s} = 1 - \beta_0\alpha_s/(4\pi\epsilon) + \mathcal{O}(\alpha_s^2)$. The soft function after the Laplace transformation can be written as

$$\begin{aligned} &\tilde{S}(L, \beta_t, \cos\theta_t, \mu) \\ &= \int_0^{\infty} d\tau \exp\left(-\frac{\tau}{e^{\gamma_E}\mu e^{L/2}}\right) S(\tau, \beta_t, \cos\theta_t, \mu) \\ &= 1 + \sum_{n=1}^{\infty}\left(\frac{Z_{\alpha_s}\alpha_s}{4\pi}\right)^n e^{-n(L+2\gamma_E)\epsilon}\Gamma(-2n\epsilon) s^{(n)}(\beta_t, \cos\theta_t)\,. \end{aligned} \tag{16}$$

Then the corresponding renormalized soft function $\tilde{s}$ is defined as

$$\tilde{s}(L, \beta_t, \cos\theta_t, \mu) = Z_s^{-1}(L, \beta_t, \cos\theta_t, \mu)\tilde{S}(L, \beta_t, \cos\theta_t, \mu)\,, \tag{17}$$

where the renormalization factor Z_s satisfies the differential equation

$$\frac{d\ln Z_s(L, \beta_t, \cos\theta_t, \mu)}{d\ln\mu} = -\gamma_s(L, \beta_t, \cos\theta_t, \mu) \tag{18}$$

with γ_s the anomalous dimension of the soft function. We will suppress the arguments of the renormalization factor, anomalous dimension and the soft function in the following text for convenience.

Given the soft anomalous dimension γ_s, following refs. [35,36], the closed expression for Z_s is derived and can be written as

$$\begin{aligned} \ln Z_s = &\frac{\alpha_s}{4\pi}\left(\frac{\gamma_s^{(0)\prime}}{4\epsilon^2} + \frac{\gamma_s^{(0)}}{2\epsilon}\right) \\ &+ \left(\frac{\alpha_s}{4\pi}\right)^2\left(-\frac{3\beta_0\gamma_s^{(0)\prime}}{16\epsilon^3} + \frac{\gamma_s^{(1)\prime} - 4\beta_0\gamma_s^{(0)}}{16\epsilon^2} + \frac{\gamma_s^{(1)}}{4\epsilon}\right) \\ &+ \mathcal{O}(\alpha_s^3). \end{aligned} \tag{19}$$

The expansion series and derivative of the soft anomalous dimension are given by

$$\gamma_s = \sum_{i=0}\left(\frac{\alpha_s}{4\pi}\right)^{i+1}\gamma_s^{(i)} \qquad \text{and} \qquad \gamma_s^{(i)\prime} = \frac{d\gamma_s^{(i)}}{d\ln\mu}\,. \tag{20}$$

From eq. (17), we obtain the renormalized NLO and NNLO soft functions in Laplace space

$$\begin{aligned} \tilde{s}^{(1)} =& \tilde{S}^{(1)} - Z_s^{(1)}\,, \\ \tilde{s}^{(2)} =& \tilde{S}^{(2)} - Z_s^{(2)} - \tilde{S}^{(1)}Z_s^{(1)} + Z_s^{(1)2} - \frac{\beta_0}{\epsilon}\tilde{S}^{(1)}\,. \end{aligned} \tag{21}$$

Since the renormalized soft function is finite, the divergent terms in the bare soft function $\tilde{S}$ is related to the renormalization factor Z_s and can be derived from the above equations.

As discussed before, the soft anomalous dimension γ_s can be derived from the independence of the cross section on the renormalization scale μ,

$$\frac{d\ln\tilde{s}}{d\ln\mu} = \gamma_s = -\frac{d\ln H}{d\ln\mu} - \frac{d\ln\tilde{B}_1}{d\ln\mu} - \frac{d\ln\tilde{B}_2}{d\ln\mu}\,, \tag{22}$$

where $\tilde{B}_i$ is the beam function in Laplace space, of which the NLO and NNLO results can be found in refs. [20–23]. And the RG equation of the beam function is exactly the same as the evolution equation of the jet function to all orders [20],

$$\frac{d\tilde{B}_i}{d\ln\mu} = \left(-\mathbf{T}_i\cdot\mathbf{T}_i\gamma_{\rm cusp}\left(\ln\frac{s_{12}}{\mu^2} + L\right) + \gamma_B^i\right)\tilde{B}_i\,, \tag{23}$$

where $\mathbf{T}_i$ is the color generator associated with the i-th parton [37,38] and the anomalous dimension γ_B^i can be found in refs. [22,23].

The RG equation for the hard function can be obtained from refs. [39,40] where the two-loop divergences have been calculated for massive scattering amplitudes in non-abelian gauge theories. It is straightforward to organize the RG equation for the hard function as

$$\begin{aligned} \frac{d\ln H}{d\ln\mu} =& (\mathbf{T}_1\cdot\mathbf{T}_1 + \mathbf{T}_2\cdot\mathbf{T}_2)\ln\frac{s_{12}}{\mu^2} - \mathbf{T}_1\cdot\mathbf{T}_3\gamma_{\rm cusp}\ln\frac{s_{13}^2}{s_{12}m_t^2} \\ &- \mathbf{T}_2\cdot\mathbf{T}_3\gamma_{\rm cusp}\ln\frac{s_{23}^2}{s_{12}m_t^2} \\ &+ 2\gamma^1 + 2\gamma^2 + 2\gamma^{\rm Q} \end{aligned} \tag{24}$$

with $s_{12} = 2p_1\cdot p_2 + i0, s_{13} = -2p_1\cdot p_3 + i0, s_{23} = -2p_2\cdot p_3 + i0$. The anomalous dimensions $\gamma^{1,2}$ and $\gamma^{\rm Q}$, associated with the initial- and final-state particles, can be found in refs. [39,40] and references therein.

Inserting eqs. (23)–(24) to eq. (22), the anomalous dimension of the soft function is obtained

$$\begin{aligned} \gamma_s =& (\mathbf{T}_1\cdot\mathbf{T}_1 + \mathbf{T}_2\cdot\mathbf{T}_2)\gamma_{\rm cusp}L + \mathbf{T}_1\cdot\mathbf{T}_3\gamma_{\rm cusp}\ln\frac{s_{13}^2}{s_{12}m_t^2} \\ &+ \mathbf{T}_2\cdot\mathbf{T}_3\gamma_{\rm cusp}\ln\frac{s_{23}^2}{s_{12}m_t^2} \\ &- 2\gamma^{\rm Q} - \gamma_B^1 - \gamma_B^2 - 2\gamma^1 - 2\gamma^2\,, \end{aligned} \tag{25}$$

of which each ingredient is available up to NNLO.

4. Techniques in calculation

In the calculation of the NLO and NNLO soft function, we have to deal with one and two soft radiations, respectively. The phase space integration is

$$\begin{aligned} &\int\frac{d^dq}{(2\pi)^d}\delta^+(q^2) \\ &= \frac{1}{(2\pi)^d}\frac{\Omega_{d-3}}{4}\int dq^+dq^-(q^+q^-)^{-\epsilon}\int_0^{\pi}d\phi_q\sin^{-2\epsilon}\phi_q \end{aligned} \tag{26}$$

$$\begin{aligned} &\int\frac{d^dq_1d^dq_2}{(2\pi)^{2d}}\delta^+(q_1^2)\delta^+(q_2^2) \\ &= \frac{1}{(2\pi)^{2d}}\frac{\Omega_{d-3}^2}{16}\int dq_1^+dq_1^-(q_1^+q_1^-)^{-\epsilon}\int dq_2^+dq_2^-(q_2^+q_2^-)^{-\epsilon} \\ &\quad d\phi_1\sin^{-2\epsilon}\phi_1 d\phi_2\sin^{-2\epsilon}\phi_2 \end{aligned} \tag{27}$$

with

$$\Omega_{d-3} = \frac{2\pi^{\frac{1}{2}-\epsilon}}{\Gamma(\frac{1}{2}-\epsilon)} = 2 - 3\zeta(2)\epsilon^2 - \frac{14\zeta(3)\epsilon^3}{3} - \frac{15}{8}\zeta(4)\epsilon^4 + O\left(\epsilon^5\right). \quad (28)$$

The ϕ angle is measured in the frame with the top quark $\phi_t = 0$. More explicitly, we choose

$$\begin{aligned} p_{3\perp} &= |p_{3\perp}|(0;0,1), \\ q_{1\perp} &= |q_{1\perp}|(0;\sin\phi_1,\cos\phi_1), \\ q_{2\perp} &= |q_{2\perp}|(\sin\phi_2\sin\beta\hat{n}_\epsilon;\sin\phi_2\cos\beta,\cos\phi_2). \end{aligned} \quad (29)$$

For the integrand involving $1/(q_1\cdot q_2)$, the phase space integration is parameterize as

$$\begin{aligned} &\int \frac{d^dq_1 d^dq_2}{(2\pi)^{2d}}\delta^+(q_1^2)\delta^+(q_2^2) \\ &= \frac{1}{(2\pi)^{2d}}\frac{\Omega_{d-3}\Omega_{d-4}}{16}\int dq_1^+ dq_1^- (q_1^+q_1^-)^{-\epsilon}\int dq_2^+ dq_2^- (q_2^+q_2^-)^{-\epsilon} \\ &\quad d\phi_1 \sin^{-2\epsilon}\phi_1 d\phi_{12}\sin^{-2\epsilon}\phi_{12} d\beta_{12}\sin^{-1-2\epsilon}\beta_{12} \end{aligned} \quad (30)$$

with

$$\Omega_{d-4} = \frac{2\pi^{-\epsilon}}{\Gamma(-\epsilon)} = \frac{-2\epsilon\pi^{-\epsilon}}{\Gamma(1-\epsilon)}. \quad (31)$$

At NLO, the measurement function is defined as

$$F(n,\bar{n},q) = \delta(q^+-\tau)\Theta(q^- - q^+) + \delta(q^- - \tau)\Theta(q^+ - q^-)\,, \quad (32)$$

where $q^+ = q\cdot n$ and $q^- = q\cdot\bar{n}$. At NNLO, the measurement function is defined as

$$\begin{aligned} F(n,\bar{n},q_1,q_2) = {} & \delta(q_1^+ + q_2^+ - \tau)\Theta(q_1^- - q_1^+)\Theta(q_2^- - q_2^+) \\ & + \delta(q_1^+ + q_2^- - \tau)\Theta(q_1^- - q_1^+)\Theta(q_2^+ - q_2^-) \\ & + \delta(q_1^- + q_2^- - \tau)\Theta(q_1^+ - q_1^-)\Theta(q_2^+ - q_2^-) \\ & + \delta(q_1^- + q_2^+ - \tau)\Theta(q_1^+ - q_1^-)\Theta(q_2^- - q_2^+). \end{aligned} \quad (33)$$

One can see that at NNLO the whole phase space is partitioned to four pieces. We label them as Region-I, Region-II, Region-III and Region-IV, respectively.

In the hemisphere with $q_i^+ = \tau_i$, we parameterize $q_i^- = \tau_i/t_i$ with $t_i \in (0,1)$ and

$$dq_i^- = dt_i\frac{\tau_i}{t_i^2}, \quad (q_i^+q_i^-)^{-\epsilon} = (\tau_i^2/t_i)^{-\epsilon}. \quad (34)$$

And then all those singularities at NLO will appear as $\tau_i^{-1-2\epsilon}$ and $t_i^{-1+\epsilon}$. In the end, we define

$$\tau_1 = \tau v, \quad \tau_2 = \tau\bar{v}, \quad (35)$$

with $\bar{v}\equiv 1-v$. We have

$$\int d\tau_1 d\tau_2 \delta(\tau-\tau_1-\tau_2) = \tau\int_0^1 dv. \quad (36)$$

If the integrands do not involve $1/(q_1\cdot q_2)$, we perform the phase space integration straightforward after the parameterization. For the integrands involving $1/(q_1\cdot q_2)$, we have

$$q_1\cdot q_2 = \frac{1}{2}\frac{\tau_1\tau_2}{t_1t_2}\left[t_2+t_1-2\sqrt{t_1t_2}\cos\phi_{12}\right], \quad (37)$$

in the Region-I or Region-III, and

$$q_1\cdot q_2 = \frac{1}{2}\frac{\tau_1\tau_2}{t_1t_2}\left[1+t_1t_2-2\sqrt{t_1t_2}\cos\phi_{12}\right], \quad (38)$$

in the Region-II or Region-IV. Here ϕ_{12} is the angle between $q_{1\perp}$ and $q_{2\perp}$.

In the Region-I and Region-III, the double-real corrections contain a new kind of singularities that appear when $t_1 = t_2$ and $\phi_{12} = 0$. Following the method in ref. [31], we change the integration variables from ϕ_2, β to ϕ_{12}, β_{12}. All dependence on ϕ_2 (such as $q_{2\perp}\cdot p_{3\perp}$) can be expressed in terms of ϕ_{12} and β_{12},

$$\cos\phi_2 = \cos\phi_1\cos\phi_{12} - \sin\phi_1\sin\phi_{12}\cos\beta_{12}. \quad (39)$$

The β_{12} angle integration can be transformed by defining $\cos\beta_{12} = 1-2x$,

$$\int_0^\pi d\beta_{12}(\sin\beta_{12})^{-1-2\epsilon} = 2^{-1-2\epsilon}\int_0^1 dx[x(1-x)]^{-1-\epsilon}. \quad (40)$$

Define $\cos\phi_{12} = 1-2z$,

$$\begin{aligned} q_1\cdot q_2 &= \frac{1}{2}\frac{\tau_1\tau_2}{t_1t_2}\left[(\sqrt{t_2}-\sqrt{t_1})^2 + 4z\sqrt{t_1t_2}\right] \\ &= \frac{1}{2}\frac{\tau_1\tau_2}{t_1t_2}\frac{(t_2-t_1)^2}{\left[(\sqrt{t_2}-\sqrt{t_1})^2+4r\sqrt{t_1t_2}\right]}. \end{aligned} \quad (41)$$

By writing in this form, we have picked out the singular part as $t_2\to t_1$. The parameter r is solved to be

$$r = \frac{(\sqrt{t_2}-\sqrt{t_1})^2(1-z)}{(\sqrt{t_2}-\sqrt{t_1})^2+4z\sqrt{t_1t_2}}, \quad (42)$$

and the Jacobian is

$$\frac{dz}{dr} = -\frac{(t_2-t_1)^2}{\left[(\sqrt{t_2}-\sqrt{t_1})^2+4r\sqrt{t_1t_2}\right]^2}. \quad (43)$$

The ϕ_{12} angular integration is given by

$$\int_0^\pi d\phi_{12}\sin^{-2\epsilon}\phi_{12} = 4^{-\epsilon}\int_0^1 dz[z(1-z)]^{-\frac{1}{2}-\epsilon} \quad (44)$$

$$= 4^{-\epsilon}\int_0^1 dr[r(1-r)]^{-\frac{1}{2}-\epsilon}\frac{|t_2-t_1|^{1-2\epsilon}}{\left[(\sqrt{t_2}-\sqrt{t_1})^2+4r\sqrt{t_1t_2}\right]^{1-2\epsilon}}. \quad (45)$$

Combined with eq. (41), we see that the singular part of $(q_1\cdot q_2)^{-1}\sim|t_2-t_1|^{-1-2\epsilon}$ and $(q_1\cdot q_2)^{-2}\sim|t_2-t_1|^{-3-2\epsilon}$. However, we find that the coefficient of $(q_1\cdot q_2)^{-2}$ is proportional to $(t_1-t_2)^2$. Now we divide the integration region of t_1, t_2 to two sectors, i.e.,

$$\begin{aligned} &1.\quad t_1 > t_2: \quad t_2 = t_1(1-w), \quad w\in(0,1), \\ &2.\quad t_1 < t_2: \quad t_1 = t_2(1-w), \quad w\in(0,1). \end{aligned} \quad (46)$$

In each sector, $|t_2-t_1|$ has a definite sign and thus is easy to deal with.

In the Region-II and Region-IV, one can carry out the same procedure as above except the relation between r and z changes to

$$r = \frac{(1-\sqrt{t_1t_2})^2(1-z)}{(1-\sqrt{t_1t_2})^2+4z\sqrt{t_1t_2}}. \quad (47)$$

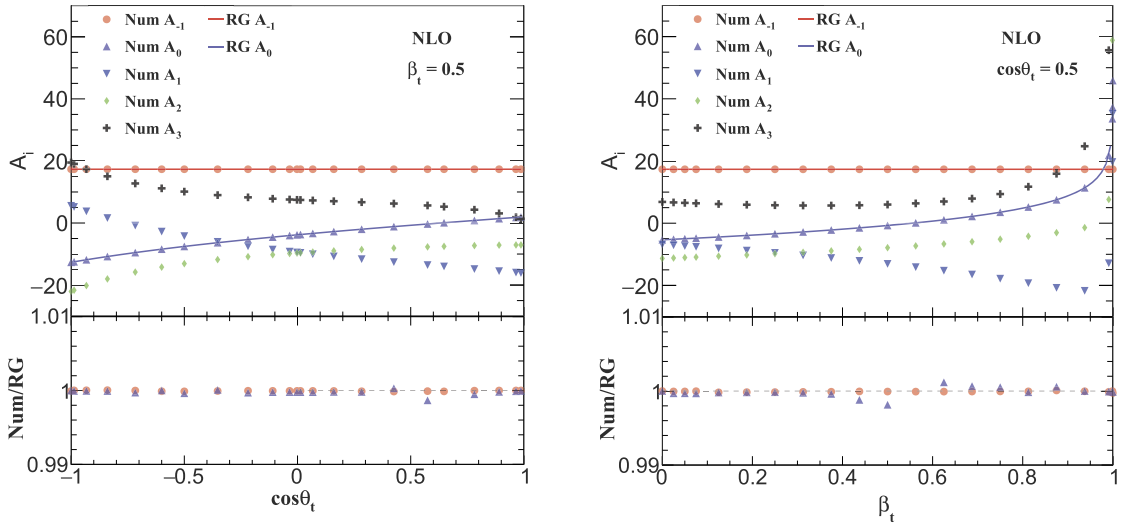

Fig. 1. Numerical results for the NLO soft function and the comparison of A_{-1} and A_0 with the RG predictions with fixed $\cos\theta_t$ (left) and β_t (right).

With this parametrization above, all the divergences can be extracted through the expansion,

$$x^{-1+n\epsilon} = \frac{1}{n\epsilon}\delta(x) + \left(\frac{1}{x}\right)_+ + n\epsilon\left(\frac{\ln x}{x}\right)_+ + \cdots . \tag{48}$$

Then all the phase space integration can be performed numerically.

5. Results of the soft function

5.1. NLO soft function

The LO soft function is trivial and has been given explicitly in eq. (15). In this section, we present its NLO result. Expanding the soft Wilson lines in eq. (11) in a series of the strong coupling, we obtain the NLO soft function

$$S^{(1)}(\tau) = \frac{2e^{\gamma_E\epsilon}\mu^{2\epsilon}}{\pi^{1-\epsilon}}\int d^dq\,\delta(q^2)\,J_a^{\mu(0)\dagger}d_{\mu\nu}(q)\,J_a^{\nu(0)}(q)F(n,\bar{n},q)\,, \tag{49}$$

where $e^{\gamma_E\epsilon}$ is inserted because we use $\overline{\rm MS}$ renormalization scheme. The factor $J_a^{\mu(0)}(q)$ is the LO one-gluon soft current, or the eikonal current,

$$J_a^{\mu(0)}(q) = \sum_{i=1}^{3}\mathbf{T}_i^a\frac{p_i^\mu}{p_i\cdot q} \tag{50}$$

with a the color index.

After performing the phase space integration, we obtain the NLO bare soft function

$$s^{(1)} = \frac{A_{-1}}{\epsilon} + A_0 + A_1\epsilon + A_2\epsilon^2 + A_3\epsilon^3 + \mathcal{O}(\epsilon^4), \tag{51}$$

where A_i is a function of β_t and $\cos\theta_t$. Fig. 1 shows the numerical results for the NLO soft function and the comparison of the divergent coefficients between the numerical calculations and RG predictions with fixed $\cos\theta_t$ or β_t. The deviations are not larger than 0.2% except for the case of $|A_i| \to 0$. The points at $\beta_t = 0$ just reproduce our previous results in ref. [32], as expected. It can also be seen that when $\beta_t \to 1$, i.e., the top quark is highly boosted, the coefficients $A_i, i = 0, 1, 2, 3$, become divergent. This is due to the logarithmic structures such as $\ln^n(1-\beta_t)$ in the limit of $\beta_t \to 1$. In principle, this kind of logarithms can be predicted from effective field theory for boosted top productions. Because the top quark mass is small compared with its energy in the limit, the scale hierarchy of the process is $\tau \ll m_t \ll \sqrt{\hat{s}}$, and thus a different factorization formula should be derived. We leave the detailed discussion to a future work. Notice that in eq. (51) and Fig. 1 we also show A_2 and A_3 which do not contribute to the NLO result. However, they will contribute to the renormalized NNLO soft function.

5.2. NNLO soft function

The NNLO contribution consists of two parts, i.e.,

$$s^{(2)} = s^{(2)}_{\rm VR} + s^{(2)}_{\rm DR}. \tag{52}$$

The first part is the virtual-real correction, i.e., the one-loop virtual corrections to LO soft gluon current $J_a^{\mu(1)}(q)$; the second part is the double-real correction, i.e., the corrections with a double-gluon soft current $J_{ab}^{\mu\nu(0)}(q_1, q_2)$ or a massless quark-pair emission. For the virtual-real contribution we use the soft limit of one-loop QCD amplitudes which has been studied in refs. [41–43] and ref. [44] for massless and massive external particles. As for the double-real contribution we make use of the results in refs. [45,46] where the infrared behaviour of tree-level QCD amplitudes at NNLO has been analyzed. The details of the virtual-real and double-real matrix element can be found in our previous paper [32].

With the techniques discussed in section 4, the double-real part is calculated numerically after sector decomposition. The bare soft function at NNLO, defined in eq. (15), can be written as

$$s^{(2)} = \frac{B_{-3}}{\epsilon^3} + \frac{B_{-2}}{\epsilon^2} + \frac{B_{-1}}{\epsilon^1} + B_0 + B_1\epsilon + \mathcal{O}(\epsilon^2)\,. \tag{53}$$

Using eq. (22) and the anomalous dimensions in eq. (25) the divergent terms in the bare NNLO soft function can be predicted, which is an important cross check of our calculations.

Table 1 shows the comparison of the divergent terms in different color structures with fixed $\beta_t = 0.3$ and $\cos\theta_t = 0.5$. We see that the maximum deviation is less than 0.2%. Figs. 2 and 3 show the numerical calculations and the RG predictions with $\cos\theta_t$ in the range of $(-1, 1)$ but fixed β_t and with β_t in the range of $(0, 1)$ but fixed $\cos\theta_t$, respectively. We find that the numerical results are consistent with the RG predictions. For most of the cases the deviations are less than 0.2%, while the deviations can be about 1% only when the absolute values of the coefficient B_i are close to

Table 1
Comparison between the numerical calculations and the RG predictions of the divergent terms in different color factors with $\beta_t = 0.3$ and $\cos\theta_t = 0.5$. In the last line, we show the maximum deviation of the numerical calculations with respect to the RG predictions.

	B_{-3}		B_{-2}		B_{-1}		B_0	
	Num	RG	Num	RG	Num	RG	Num	RG
C_A^2	−8.0000	−8	2.4972	2.4968	84.3749	84.3784	147.222	147.233
C_F^2	−8.0004	−8	19.6943	19.6916	26.6838	26.6908	64.0611	63.9972
$C_A C_F$	−16.0000	−16	22.1903	22.1885	107.408	107.386	194.270	194.217
$C_A n_f$	0	0	−1.3332	−1.3333	−3.0273	−3.0283	3.2803	3.2779
$C_F n_f$	0	0	−1.3335	−1.3333	1.0599	1.0597	−1.0928	−1.0949
Max.devi.	5×10^{-5}		1.5×10^{-4}		3.5×10^{-4}		1.3×10^{-3}	

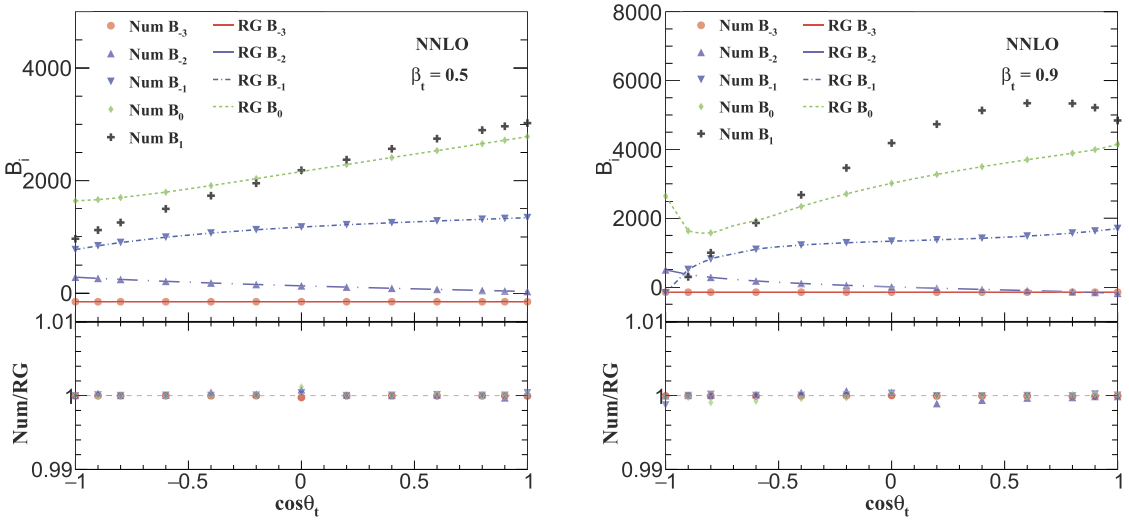

Fig. 2. Numerical results for NNLO bare soft function and the comparison to the RG predictions with $\beta_t = 0.5$ (left) and 0.9 (right). The color factors are $C_A = 3$ and $C_F = 4/3$ and the number of flavors is $n_f = 5$. (For interpretation of the colors in the figure(s), the reader is referred to the web version of this article.)

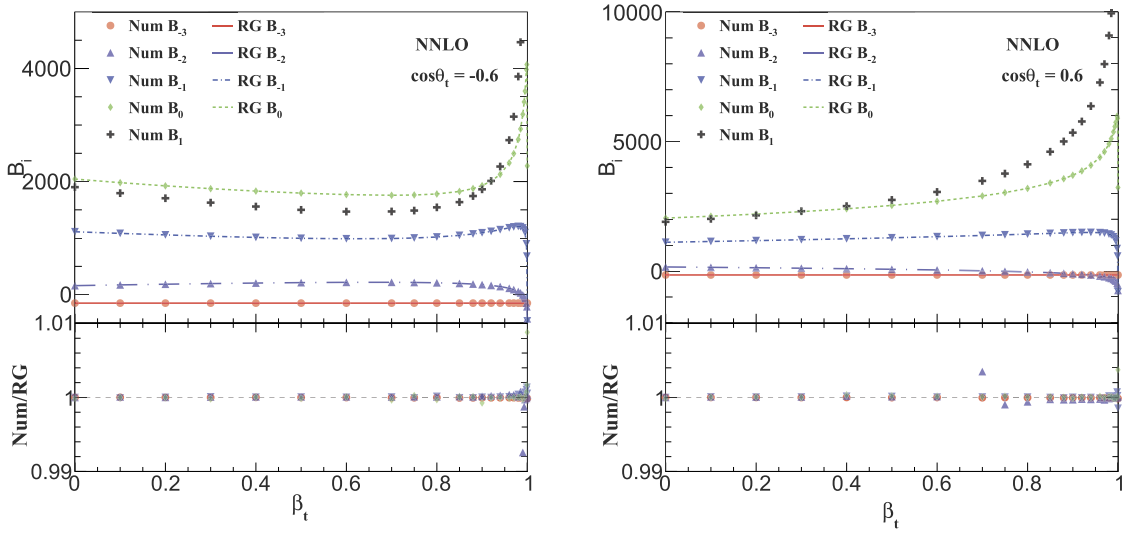

Fig. 3. Numerical results for NNLO bare soft function and the comparison to the RG predictions with $\cos\theta_t = -0.6$ (left) and 0.6 (right). The color factors are $C_A = 3$ and $C_F = 4/3$ and the number of flavors is $n_f = 5$.

zero. We have checked that the points at $\beta_t = 0$ reproduce our previous results in ref. [32]. Similar to the NLO results, in the highly boosted region, the NNLO coefficients contains logarithmic structures such as $\ln^n(1-\beta_t)$. They are divergent when $\beta_t \to 1$. This fact explains the behaviour of the distributions of the points near the end point of β_t in Fig. 3.

6. Conclusions

The N-jettiness subtraction method is one of the efficient methods to perform differential calculations of the NNLO cross sections. In this paper, we present the calculation of NNLO soft function for one massive colored particle production which is one of the indispensable ingredients in N-jettiness subtraction method. Our calculation makes use of the one-loop soft current and infrared limit of the QCD matrix elements from refs. [43–46] to construct the integrand. The phase space integrations are performed with the sector decomposition method and the techniques are discussed in details. The divergent terms of NLO and NNLO soft functions in our calculations are in very good agreement with those from the RG predictions. Though our result is general for a single massive colored particle production, we focus on tW production in the discussion because it is one of the most important processes in the SM. Once the two-loop hard function is obtained, we can perform the NNLO calculation for the differential cross section of tW production at hadron colliders. Our method can also be applied to the calculation of the N-jettiness soft function for top quark pair production, which provides another way to study the NNLO differential cross section for this process. We leave this application in future study.

Acknowledgements

HTL would like to acknowledge the TU Munich for its hospitality during the completion of this work. We thank Xiaohui Liu for useful discussion. The work of HTL was supported by Department of Energy Early Career Program. The work of JW was supported by the BMBF project No. 05H15WOCAA.

References

[1] G. Heinrich, QCD calculations for the LHC: status and prospects, in: 5th Large Hadron Collider Physics Conference, (LHCP 2017) Shanghai, China, May 15–20, 2017, 2017, arXiv:1710.04998.
[2] R. Boughezal, C. Focke, X. Liu, F. Petriello, W-boson production in association with a jet at next-to-next-to-leading order in perturbative QCD, Phys. Rev. Lett. 115 (6) (2015) 062002, arXiv:1504.02131.
[3] J. Gaunt, M. Stahlhofen, F.J. Tackmann, J.R. Walsh, N-jettiness Subtractions for NNLO QCD Calculations, J. High Energy Phys. 09 (2015) 058, arXiv:1505.04794.
[4] R. Boughezal, C. Focke, W. Giele, X. Liu, F. Petriello, Higgs boson production in association with a jet at NNLO using jettiness subtraction, Phys. Lett. B 748 (2015) 5–8, arXiv:1505.03893.
[5] R. Boughezal, J.M. Campbell, R.K. Ellis, C. Focke, W.T. Giele, X. Liu, F. Petriello, Z-boson production in association with a jet at next-to-next-to-leading order in perturbative QCD, Phys. Rev. Lett. 116 (15) (2016) 152001, arXiv:1512.01291.
[6] J.M. Campbell, R.K. Ellis, C. Williams, Direct photon production at next-to–next-to-leading order, Phys. Rev. Lett. 118 (22) (2017) 222001, arXiv:1612.04333.
[7] C.W. Bauer, S. Fleming, M.E. Luke, Summing Sudakov logarithms in $B \to X_s$ gamma in effective field theory, Phys. Rev. D 63 (2000) 014006, arXiv:hep-ph/0005275.
[8] C.W. Bauer, S. Fleming, D. Pirjol, I.W. Stewart, An effective field theory for collinear and soft gluons: heavy to light decays, Phys. Rev. D 63 (2001) 114020, arXiv:hep-ph/0011336.
[9] C.W. Bauer, I.W. Stewart, Invariant operators in collinear effective theory, Phys. Lett. B 516 (2001) 134–142, arXiv:hep-ph/0107001.
[10] C.W. Bauer, D. Pirjol, I.W. Stewart, Soft-collinear factorization in effective field theory, Phys. Rev. D 65 (2002) 054022, arXiv:hep-ph/0109045.
[11] M. Beneke, A.P. Chapovsky, M. Diehl, T. Feldmann, Soft collinear effective theory and heavy to light currents beyond leading power, Nucl. Phys. B 643 (2002) 431–476, arXiv:hep-ph/0206152.
[12] I.W. Stewart, F.J. Tackmann, W.J. Waalewijn, N-jettiness: an inclusive event shape to veto jets, Phys. Rev. Lett. 105 (2010) 092002, arXiv:1004.2489.
[13] I.W. Stewart, F.J. Tackmann, W.J. Waalewijn, Factorization at the LHC: from PDFs to initial state jets, Phys. Rev. D 81 (2010) 094035, arXiv:0910.0467.
[14] J. Gao, C.S. Li, H.X. Zhu, Top quark decay at next-to-next-to leading order in QCD, Phys. Rev. Lett. 110 (4) (2013) 042001, arXiv:1210.2808.
[15] E.L. Berger, J. Gao, C.P. Yuan, H.X. Zhu, NNLO QCD corrections to t-channel single top-quark production and decay, Phys. Rev. D 94 (7) (2016), arXiv:1606.08463.
[16] G. Heinrich, S. Jahn, S.P. Jones, M. Kerner, J. Pires, NNLO predictions for Z-boson pair production at the LHC, arXiv:1710.06294.
[17] E.L. Berger, J. Gao, C.S. Li, Z.L. Liu, H.X. Zhu, Charm-quark production in deep-inelastic neutrino scattering at next-to-next-to-leading order in QCD, Phys. Rev. Lett. 116 (21) (2016) 212002, arXiv:1601.05430.
[18] G. Abelof, R. Boughezal, X. Liu, F. Petriello, Single-inclusive jet production in electron–nucleon collisions through next-to-next-to-leading order in perturbative QCD, Phys. Lett. B 763 (2016) 52–59, arXiv:1607.04921.
[19] S. Alioli, C.W. Bauer, C.J. Berggren, A. Hornig, F.J. Tackmann, C.K. Vermilion, J.R. Walsh, S. Zuberi, Combining higher-order resummation with multiple NLO calculations and parton showers in Geneva, J. High Energy Phys. 09 (2013) 120, arXiv:1211.7049.
[20] I.W. Stewart, F.J. Tackmann, W.J. Waalewijn, The quark beam function at NNLL, J. High Energy Phys. 09 (2010) 005, arXiv:1002.2213.
[21] C.F. Berger, C. Marcantonini, I.W. Stewart, F.J. Tackmann, W.J. Waalewijn, Higgs production with a central jet veto at NNLL+NNLO, J. High Energy Phys. 04 (2011) 092, arXiv:1012.4480.
[22] J.R. Gaunt, M. Stahlhofen, F.J. Tackmann, The quark beam function at two loops, J. High Energy Phys. 04 (2014) 113, arXiv:1401.5478.
[23] J. Gaunt, M. Stahlhofen, F.J. Tackmann, The gluon beam function at two loops, J. High Energy Phys. 08 (2014) 020, arXiv:1405.1044.
[24] T. Becher, M. Neubert, Toward a NNLO calculation of the anti-B $\to X_s$ gamma decay rate with a cut on photon energy. II. Two-loop result for the jet function, Phys. Lett. B 637 (2006) 251–259, arXiv:hep-ph/0603140.
[25] T. Becher, G. Bell, The gluon jet function at two-loop order, Phys. Lett. B 695 (2011) 252–258, arXiv:1008.1936.
[26] T.T. Jouttenus, I.W. Stewart, F.J. Tackmann, W.J. Waalewijn, The soft function for exclusive N-jet production at hadron colliders, Phys. Rev. D 83 (2011) 114030, arXiv:1102.4344.
[27] R. Kelley, M.D. Schwartz, R.M. Schabinger, H.X. Zhu, The two-loop hemisphere soft function, Phys. Rev. D 84 (2011) 045022, arXiv:1105.3676.
[28] P.F. Monni, T. Gehrmann, G. Luisoni, Two-loop soft corrections and resummation of the thrust distribution in the dijet region, J. High Energy Phys. 08 (2011) 010, arXiv:1105.4560.
[29] R. Boughezal, X. Liu, F. Petriello, N-jettiness soft function at next-to-next-to-leading order, Phys. Rev. D 91 (9) (2015) 094035, arXiv:1504.02540.
[30] D. Kang, O.Z. Labun, C. Lee, Equality of hemisphere soft functions for e^+e^-, DIS and pp collisions at $\mathcal{O}(\alpha_s^2)$, Phys. Lett. B 748 (2015) 45–54, arXiv:1504.04006.
[31] J.M. Campbell, R.K. Ellis, R. Mondini, C. Williams, The NNLO QCD soft function for 1-jettiness, arXiv:1711.09984.
[32] H.T. Li, J. Wang, Next-to-next-to-leading order N-jettiness soft function for one massive colored particle production at hadron colliders, J. High Energy Phys. 02 (2017) 002, arXiv:1611.02749.
[33] J. Chay, C. Kim, Y.G. Kim, J.-P. Lee, Soft Wilson lines in soft-collinear effective theory, Phys. Rev. D 71 (2005) 056001, arXiv:hep-ph/0412110.
[34] G.P. Korchemsky, A.V. Radyushkin, Infrared factorization, Wilson lines and the heavy quark limit, Phys. Lett. B 279 (1992) 359–366, arXiv:hep-ph/9203222.
[35] T. Becher, M. Neubert, Infrared singularities of scattering amplitudes in perturbative QCD, Phys. Rev. Lett. 102 (2009) 162001, arXiv:0901.0722;
T. Becher, M. Neubert, Phys. Rev. Lett. 111 (19) (2013) 199905, Erratum.
[36] T. Becher, M. Neubert, On the structure of infrared singularities of gauge-theory amplitudes, J. High Energy Phys. 06 (2009) 081, arXiv:0903.1126.
[37] S. Catani, M.H. Seymour, The Dipole formalism for the calculation of QCD jet cross-sections at next-to-leading order, Phys. Lett. B 378 (1996) 287–301, arXiv:hep-ph/9602277.
[38] S. Catani, M.H. Seymour, A general algorithm for calculating jet cross-sections in NLO QCD, Nucl. Phys. B 485 (1997) 291–419, arXiv:hep-ph/9605323;
S. Catani, M.H. Seymour, Nucl. Phys. B 510 (1998) 503, Erratum.
[39] A. Ferroglia, M. Neubert, B.D. Pecjak, L.L. Yang, Two-loop divergences of scattering amplitudes with massive partons, Phys. Rev. Lett. 103 (2009) 201601, arXiv:0907.4791.
[40] A. Ferroglia, M. Neubert, B.D. Pecjak, L.L. Yang, Two-loop divergences of massive scattering amplitudes in non-abelian gauge theories, J. High Energy Phys. 11 (2009) 062, arXiv:0908.3676.
[41] Z. Bern, V. Del Duca, C.R. Schmidt, The Infrared behavior of one loop gluon amplitudes at next-to-next-to-leading order, Phys. Lett. B 445 (1998) 168–177, arXiv:hep-ph/9810409.
[42] Z. Bern, V. Del Duca, W.B. Kilgore, C.R. Schmidt, The infrared behavior of one loop QCD amplitudes at next-to-next-to leading order, Phys. Rev. D 60 (1999) 116001, arXiv:hep-ph/9903516.

[43] S. Catani, M. Grazzini, The soft gluon current at one loop order, Nucl. Phys. B 591 (2000) 435–454, arXiv:hep-ph/0007142.
[44] I. Bierenbaum, M. Czakon, A. Mitov, The singular behavior of one-loop massive QCD amplitudes with one external soft gluon, Nucl. Phys. B 856 (2012) 228–246, arXiv:1107.4384.
[45] S. Catani, M. Grazzini, Infrared factorization of tree level QCD amplitudes at the next-to-next-to-leading order and beyond, Nucl. Phys. B 570 (2000) 287–325, arXiv:hep-ph/9908523.
[46] M. Czakon, Double-real radiation in hadronic top quark pair production as a proof of a certain concept, Nucl. Phys. B 849 (2011) 250–295, arXiv:1101.0642.